AD-A051 289 MISSION RESEARCH CORP SANTA BARBARA CALIF F/G 20/14
AXISYMMETRIC DAMPING OF CYLINDRICAL CAVITY MODES BY SHEET DAMPE--ETC(U)
AUG 77 R STETTNER, R MARKS DNA001-77-C-0009
UNCLASSIFIED MRC-R-328 DNA-4378T NL

END
DATE FILMED
4 -78
DDC

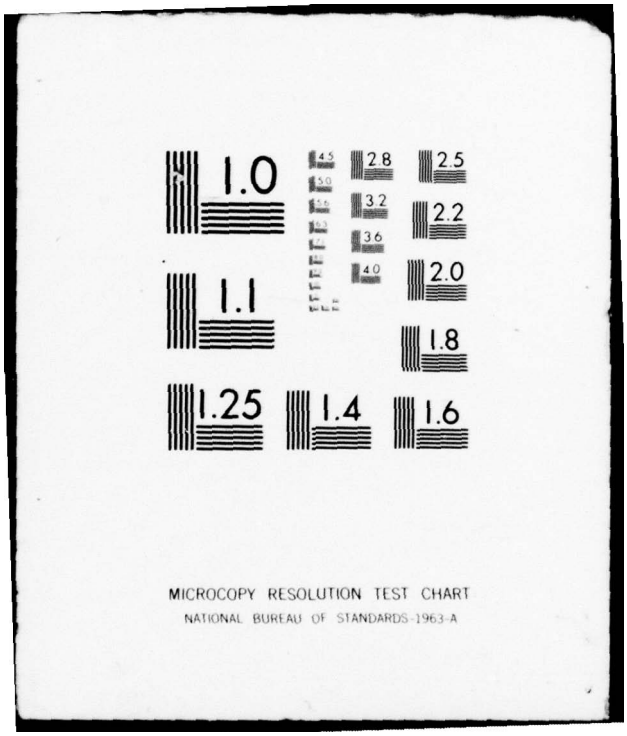
1.0
1.1
1.25
1.4
1.6
1.8
2.0
2.2
2.5
2.8
3.2
3.6
4.0
4.5
5.0
MICROCOPY RESOLUTION TEST CHART
NATIONAL BUREAU OF STANDARDS-1963-A

DNA 4378T

AXISYMMETRIC DAMPING OF CYLINDRICAL CAVITY MODES BY SHEET DAMPERS

(10)

Mission Research Corporation
735 State Street
Santa Barbara, California 93101

August 1977

Topical Report

CONTRACT No. DNA 001-77-C-0009

THIS WORK SPONSORED BY THE DEFENSE NUCLEAR AGENCY
UNDER RDT&E RMSS CODE B323077464 R99QAXEE50104 H2590D.

Prepared for
Director
DEFENSE NUCLEAR AGENCY
Washington, D. C. 20305

Destroy this report when it is no longer needed. Do not return to sender.

(18) DNA, SBIE (19) 4378T, AD-E300 101

UNCLASSIFIED

SECURITY CLASSIFICATION OF THIS PAGE (When Data Entered)

REPORT DOCUMENTATION PAGE

READ INSTRUCTIONS BEFORE COMPLETING FORM

1. REPORT NUMBER: DNA 4378T
2. GOVT ACCESSION NO.
3. RECIPIENT'S CATALOG NUMBER

4. TITLE (and Subtitle): (6) AXISYMMETRIC DAMPING OF CYLINDRICAL CAVITY MODES BY SHEET DAMPERS.

5. TYPE OF REPORT & PERIOD COVERED: (9) Topical Report

6. PERFORMING ORG. REPORT NUMBER: (14) MRC-R-328

7. AUTHOR(s): (10) Roger Stettner, Robert Marks

8. CONTRACT OR GRANT NUMBER(s): (15) DNA 001-77-C-0009

9. PERFORMING ORGANIZATION NAME AND ADDRESS
Mission Research Corporation
735 State Street
Santa Barbara, California 93101

10. PROGRAM ELEMENT, PROJECT, TASK AREA & WORK UNIT NUMBERS
NWED Subtask
(16) R99QAXEE501-04 (17) E501

11. CONTROLLING OFFICE NAME AND ADDRESS
Director
Defense Nuclear Agency
Washington, D. C. 20305

12. REPORT DATE: (11) Aug 77

13. NUMBER OF PAGES: 42 (12) 44p

14. MONITORING AGENCY NAME & ADDRESS(if different from Controlling Office)

15. SECURITY CLASS (of this report): UNCLASSIFIED

15a. DECLASSIFICATION/DOWNGRADING SCHEDULE

16. DISTRIBUTION STATEMENT (of this Report)

Approved for public release; distribution unlimited.

17. DISTRIBUTION STATEMENT (of the abstract entered in Block 20, if different from Report)

18. SUPPLEMENTARY NOTES

This work sponsored by the Defense Nuclear Agency under RDT&E RMSS Code B323077464 R99QAXEE50104 H2590D.

19. KEY WORDS (Continue on reverse side if necessary and identify by block number)

Cavity Mode Damper
Resistive Sheet Damper
Resonant Cavities

20. ABSTRACT (Continue on reverse side if necessary and identify by block number)

The equations for a two-sheet cylindrical, resistive damper, with no end caps, are derived for TM cylindrical cavity modes. These equations are solved in first order. Optimum damper position, resistance, and cavity Q are discussed in light of this solution.

DD FORM 1 JAN 73 1473 EDITION OF 1 NOV 65 IS OBSOLETE

UNCLASSIFIED

SECURITY CLASSIFICATION OF THIS PAGE (When Data Entered)

406 548

CONTENTS

		PAGE
ILLUSTRATIONS		2
TABLES		4
SECTION		
1	INTRODUCTION	5
2	HEURISTIC ANALYSIS OF MEMBRANE DAMPER	7
3	THEORY	
	3.1 ONE AND TWO SHEET DAMPERS IN THE FORM OF A CYLINDER WITH OPEN ENDS	12
	3.2 AN APPROXIMATION FOR ONE AND TWO SHEET DAMPERS	17
4	RESULTS	21
5	CONCLUSIONS	37
REFERENCES		38

ILLUSTRATIONS

FIGURE		PAGE
1	Cross section of a cylinder with membranes.	14
2	Optimum resistance vs. α, for $p = 0$, $n \leq 5$.	22
3	Optimum resistance vs. α, $p = 5$, $n \leq 5$.	22
4	Optimum resistance vs. α, $p = 10$, $n = 5$.	23
5	δ^I_{10} vs. α.	23
6	δ^I_{20} vs. α.	24
7	δ^I_{30} vs. α.	24
8	δ^I_{40} vs. α.	25
9	δ^I_{50} vs. α.	25
10	δ^I_{12} vs. α.	26
11	δ^I_{22} vs. α.	26
12	δ^I_{32} vs. α.	27
13	δ^I_{42} vs. α.	27
14	δ^I_{52} vs. α.	28
15	δ^I_{15} vs. α.	28
16	$^I_{25}$ vs. α.	29

FIGURE		PAGE
17	δ^{I}_{35} vs. α.	29
18	δ^{I}_{45} vs. α.	30
19	δ^{I}_{55} vs. α.	30
20	U_{np} vs. z_{np}.	36

TABLES

TABLE		PAGE
1	Q(n,p) for two damper sheets at α = .8 and α = .92.	33
2	X_n/δ^I_{np} for two damper sheets at α = .8 and α = .92.	33
3	Damping time T_{np} for TM cylindrical tank modes (in nanoseconds).	34
4	Optimum resistance (ohms) for sheet at α = .8.	34
5	Optimum resistance (ohms) for sheet at α = .92.	35

SECTION 1
INTRODUCTION

One of the most undesirable concomitants of simulating SGEMP in a vacuum tank is that cavity oscillations are excited. Because the Q (Q is defined as the number of periods necessary for the energy to decay to e^{-1} times its initial value) of these tanks is much larger than 1, the cavity oscillations can interfere with the experiment for the entire duration of the data taking, after a time interval equal to the clear time of the tank. To rid the experiment of these oscillations a number of dampers have been suggested. In analyzing the effect of these dampers different methods have been used. This report will concern itself with, hopefully, elucidating the effect of one of these types of dampers using a modal-type analysis.

A damper which is inexpensive and easy to construct (relative to other types of dampers) is the membrane damper. M. Messier[1] has evaluated the effect of a one and two sheet, membrane damper using a reflection coefficient analysis. Although this type of analysis does not directly utilize the concept of energy absorption in the membrane the reflection coefficient analysis has been shown, by M. A. Messier,[2] to be nearly equivalent to an analysis which does use the concept of energy absorption. Nevertheless, it is important to describe "how" the membrane damper actually damps modal oscillations. In this report we first investigate how the damper works by some heuristic arguments and then a more exact analysis is done. These heuristic arguments will be made in Section 2. The more exact analysis is made for a one or two sheet damper, and can be used to evaluate

the transverse magnetic mode damping for a cylindrical tank. This latter analysis is contained in Section 3 and is based upon modal arguments similar to those of W. A. Seidler[3] and C. Baum.[4] In Section 3, our derivation of the more exact equations for a damper analysis will assume that the damper sheets are cylinders with no end caps. (The heuristic analysis suggests that end caps might decrease the Q of the tank by a factor proportional to the area of the end caps, for modes which have an electric field in the radial direction.)

Part of the conclusions which can be drawn from the heuristic analysis of Section 2 are based upon assuming that the modes of the tank are not appreciably changed by the damper sheets. Although the relations derived in Section 2 show how the variation of parameters effect damping, they can't really be used to design a damper; the relations are too inaccurate. In Section 3.2 we make a first order approximation, to the exact equations derived in Section 3.1, to obtain an accurate approximation of the relationship between modes, damper positions and sheet resistance. The first order approximation is based on assuming that the modes do not appreciably change when damper sheets are introduced in the tank.

In Section 4 the results of Sections 2 and 3 are compared and further conclusions are drawn. Graphs and tables are presented that should be useful in designing sheet dampers. Finally in Section 5 we summarize our results and conclusions.

SECTION 2
HEURISTIC ANALYSIS OF MEMBRANE DAMPER

We shall try to show, in a somewhat heuristic way, what physics goes into a sheet damper analysis; the sheet damper is contrasted with damping due to cavity walls of finite conductivity. In our analysis, we will demonstrate what parameters the Q of the cavity depends upon. We will also get a ball park numerical answer for sheet resistance. We explicitly consider only one damper sheet. If $\mathscr{E}$ is the energy in a cavity then the rate of change of the energy is the Joule heat loss:

$$\frac{d\mathscr{E}}{dt} = -\int \vec{J} \cdot \vec{E} dV \ , \tag{1}$$

where $\vec{J}$ is the current in the sheet and $\vec{E}$ is the electric field in the sheet. If A is the area of the sheet, d its thickness, σ its conductivity and $E_{\parallel}$ the field parallel to the sheet then

$$\frac{d\mathscr{E}}{dt} = - Ad\sigma E_{\parallel}^2 \ , \tag{2}$$

where we have assumed that the current in the sheet is related to $\vec{E}$ by

$$\vec{J} = \sigma \vec{E} \ ,$$

and that $\vec{E}$ is roughly constant over the thickness d. This latter condition is satisfied if

$$\frac{\delta}{d} = \frac{c}{2\pi} \sqrt{\frac{\tau R_e}{d}} >> 1 \ , \tag{3}$$

where δ is the skin depth for a mode which has the period τ and a sheet whose resistance is R_e(sec/cm).

To relate the parameters in Equation 2 to the Q of the cavity we must relate $E_{\shortparallel}^2$ to the energy in the cavity. In general

$$\mathscr{E} = 2VE^2 \ , \tag{4}$$

where V is the volume of the cavity. Also, we may have

$$E_{\shortparallel}^2 \simeq E^2 \ . \tag{5}$$

Combining Equations 4, 5 and 2 we find

$$\frac{d\mathscr{E}}{dt} = -\frac{1}{2}\left(\frac{Ad}{V}\right)\sigma\mathscr{E} \ . \tag{6}$$

Defining the Q of the cavity as the number of periods, τ, for the energy to decay to e^{-1} of its initial value, we find that

$$Q = \left(\frac{2}{\sigma\tau}\right)\left(\frac{V}{Ad}\right) \ , \tag{7}$$

where

$$\frac{d\mathscr{E}}{dt} = -\frac{1}{Q\tau}\mathscr{E} \ , \tag{8}$$

if the damper does not charge the period appreciably. For a cylindrical cavity, of radius R the period τ of the 1st mode can be approximated by

$$\tau \simeq \frac{2.4R}{c} \ . \tag{9}$$

Substituting (9) into (7) we find that the Q for the 1st mode is approximated by

$$Q \simeq \frac{1}{2.4}\left(\frac{R}{R_0}\right) cR_e \ , \tag{10}$$

where we have made use of the relations

$$V = \pi R^2 h \ , \tag{11}$$

$$A = 2\pi R_0 h \ , \tag{12}$$

$$R_e = (\sigma d)^{-1} \quad . \tag{13}$$

In Equation 12 we have assumed that the area of the damper comes from a cylindrical sheet of radius R_0 with no end caps. Equation 10 is the equation we are seeking.

We can obtain a ball park estimate of the sheet resistance R_e from Equation 10:

$$R_e = 2.4 \frac{Q}{c} \left(\frac{R_0}{R}\right) \frac{\text{sec}}{\text{cm}}$$

$$= 72\ Q \left(\frac{R_0}{R}\right) (\text{ohm}) \ , \tag{14}$$

if $R_0/R = .8$ and $Q = 1$ then R_e is 58 ohms. That is we should expect a sheet resistance of the order of 100 ohms. Q equal to 1 is about the smallest value Q can have without appreciably changing the period of the mode; R_0/R equal to 18 is a convenient position for the damper.

Equation 10 suggests that the Q can be made smaller by reducing the resistance R_e or increasing the sheet position radius R_0. The actual relationship between R_0, R_e and Q for a given mode, however, depends upon how the fields actually vary with position in the cavity and is more complex than Equation 10. (For example, in the present discussion we assumed that the electric field parallel to the damper is constant in the cavity, whereas, in fact, it vanishes at the walls of the cavity.) With an accurate calculation Q is minimized with respect to R_0 and R_e.

We can get an impression of how end caps on the conducting sheet might affect the damping by investigating Equation 7. From Equation 7 we see that the Q of a cavity is inversely proportional to the area. The ratio of the area of a cylinder with end caps to one with no end caps is $(1 + R/h)$. For h equal to 6 meters and R equal to 2 meters this ratio would be 4/3. A damper which was a complete cylinder might have a Q about 25 percent smaller

than a damper which has no end caps. This latter statement has meaning only for modes which have electric fields in the radial direction; in general the energy in the radial electric field should be about equal to the energy associated with the electric field in the z direction.

From Equation 10, we can understand how sheet damping differs from that of damping due to the walls of the tank alone. If $R_0 = .8R$, in Equation 10, then

$$Q \cong .33\ cR_e \ . \tag{15}$$

From Reference 5 the Q for the lowest mode of a cavity, $\overline{Q}$, whose length is three times its radius is

$$\overline{Q} = \frac{3}{8\pi}\frac{R}{\overline{\delta}} \ . \tag{16}$$

Equation 16 expresses the Q for a cavity whose damping depends only on the finite conductivity of its walls. A bar over a quantity will refer to this latter cavity. $\overline{\delta}$ is the skin depth and is given by

$$\overline{\delta} = \frac{c}{2\pi}\sqrt{\frac{\tau}{\sigma}} \ . \tag{17}$$

Using Equation 9 to approximate $\overline{\delta}$ we have

$$\overline{\delta} \sim \frac{1}{4}\sqrt{\frac{Rc}{\overline{\delta}}} \ . \tag{18}$$

Substituting (18) into (16) we find that

$$\overline{Q} \simeq (.48)\ \frac{\overline{\sigma}R}{c} \ . \tag{19}$$

If we define an effective "sheet resistance" by

$$\overline{R}_e = \frac{1}{\overline{\sigma}R} \ , \tag{20}$$

then

$$\overline{Q} \simeq .48\ (\overline{R}_e c)^{-1/2} \quad . \tag{21}$$

Increasing the conductivity or decreasing the sheet resistance has the opposite effect for the two types of damping. The difference between Equations 15 and 21 arises because Equation 20 is really a second order effect. That is, the E fields parallel to the cavity wall are assumed to be zero in first order. Damping at the walls appears because the E fields at walls are not quite parallel to the walls. Equation 15 is the result of a first order calculation; that is the E field parallel to the damper is non-zero in first order.

SECTION 3

THEORY

3.1 ONE AND TWO SHEET DAMPERS IN THE FORM OF A CYLINDER WITH OPEN ENDS

In this section we derive the mathematical relationship which relates the position of the damper sheets and their conductivity to the complex frequencies of the cavity. The frequencies are complex because the damper sheets have introduced modal damping. This damping appears in the mathematics as an imaginary part of the new modal frequency. We begin by assuming that we have a cavity in which axisymmetric modes have been established. The cavity, except for the membranes, is empty. The membranes will be assumed to be open ended cylinders; only two membranes will be considered.

Figure 1 depicts the physical situation. The membranes are treated as boundaries between regions I, II and III. In these three, source free regions, Maxwell's equations are

$$\frac{\partial}{\partial r}\left(\frac{1}{r}\frac{\partial}{\partial r}\,rB\right) + \frac{\partial^2 B}{\partial z^2} - \frac{1}{c^2}\frac{\partial^2 B}{\partial t^2} = 0 \ , \tag{22}$$

$$\frac{1}{c}\frac{\partial E_r}{\partial t} = -\frac{\partial B}{\partial z} \ , \tag{23}$$

and

$$\frac{1}{c}\frac{\partial E_z}{\partial t} = \frac{1}{r}\frac{\partial}{\partial r}\,(rB) \ , \tag{24}$$

where a subscript z or r refers to the z or r cylindrical coordinates respectively, E and B refer to electric and magnetic respectively. Assuming that the time dependence can be represented by $e^{i\omega t}$ and defining $k^2 \equiv (\omega/c)^2 - (p\pi/L)^2$ we can solve for the fields in the three regions in terms of a series of Bessel functions and the trigonometric functions $\sin(p\pi z/L)$ and $\cos(p\pi z/L)$; where p is an integer and L is the height of the cavity. Since this analysis is not really dependent upon the trigonometric functions we suppress them in the equations to follow.

We are really interested in computing the frequencies of oscillation of the system depicted in Figure 1. To do so we must match the solutions in the various regions across the membranes and then finally require E_z to be equal to zero at the tank wall. In region I the solution is

$$B_I = \mathcal{A} J_1(kr) \ , \tag{25}$$

and from Equations 24 and 25

$$E_{Iz} = -\mathcal{A} \frac{ck}{\omega} iJ_0(kr) \ . \tag{26}$$

The symbol $\mathcal{A}$ in Equations 4 and 5 represents a constant to be determined; the subscript I represents region I. J_q are Bessel functions of order q. In region II the fields are

$$B_{II} = eJ_1(kr) + bN_1(kr) \ , \tag{27}$$

and

$$E_{II\,z} = -i(eJ_0(kr) + bN_0(kr))ck/\omega \ , \tag{28}$$

where e and b are constants to be determined and N_q is a Neuman function of order q. In region III the fields are

$$B_{III} = J_1(kr) + fN_1(kr) \ , \tag{29}$$

and

$$E_{III\,z} = -i(J_0(kr) + fN_0(kr))ck/\omega \ . \tag{30}$$

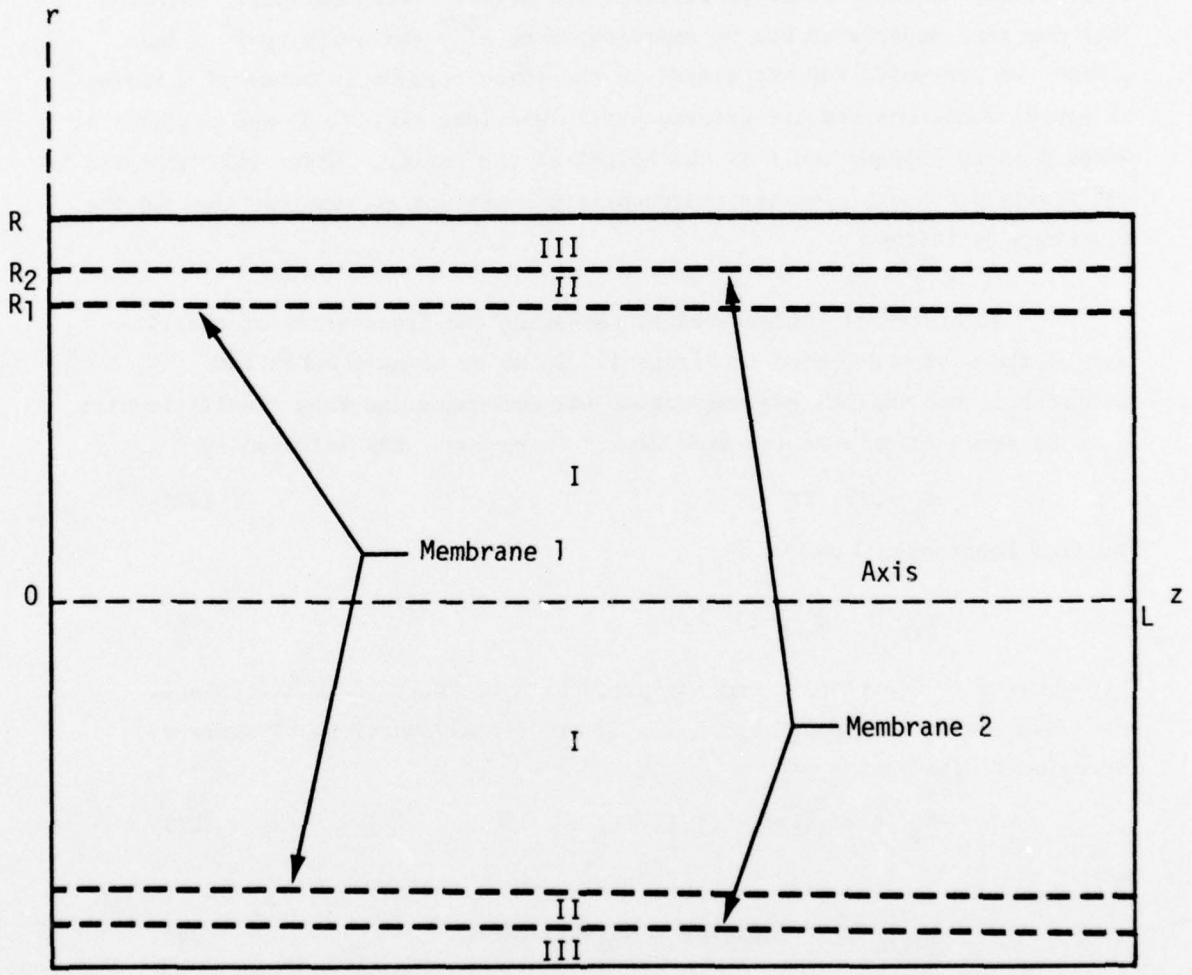

Figure 1. Cross section of a cylinder with membranes.

To find the four constants a, b, e, and f we apply the boundary conditions across membranes 1 and 2. The boundary conditions are:

$$B_{II} - B_I = 4\pi E_z/c\, R_{e1}\ ,\quad r = R_1\ , \tag{31}$$

$$E_{II\,z} = E_{1\,z}\ ,\ \text{at } r = R_1\ , \tag{32}$$

for membrane 1 and

$$B_{III} - B_{II} = 4\pi E_z/c\, R_{e2}\ ,\ r = R_1\ , \tag{33}$$

$$E_{III\,z} = E_{II\,z}\ ,\ \text{at } r = R_2\ , \tag{34}$$

for membrane 2, where R_{eq} is the sheet resistance of membrane q. Inserting Equations 25 through 30 into Equations 31 through 33 we end up with the four equations

$$fa_{11} + ea_{12} + ba_{13} = h_1\ , \tag{35}$$

$$fa_{21} + ea_{22} + ba_{23} = h_2\ , \tag{36}$$

$$ea_{32} + ba_{33} + aa_{31} = 0\ , \tag{37}$$

$$ea_{42} + ba_{43} + aa_{44} = 0\ , \tag{38}$$

where

$$\left.\begin{aligned}
&a_{11} = -N_1(x\alpha_2), a_{12} = J_1(x\alpha_2) - z_2 J_0(x\alpha_2)\\
&a_{13} = N_1(x\alpha_2) - z_2 n_0(x\alpha_2), h_1 = J_1(x\alpha_2)\\
&a_{21} = -N_0(x\alpha_2), a_{22} = J_0(x\alpha_2)\\
&a_{23} = N_0(x\alpha_2), h_2 = J_0(x\alpha_2)\\
&a_{32} = J_1(x\alpha_1), a_{33} = N_1(x\alpha_1)\\
&a_{34} = z_1 J_0(x\alpha_1) - J_1(x\alpha_1)\\
&a_{42} = -J_0(x\alpha_1), a_{43} = -N_0(x\alpha_1)\\
&a_{44} = J_0(x\alpha_1)\ ,
\end{aligned}\right\} \tag{39}$$

and where we have used the definition:

$$kR \equiv x \ , \tag{40}$$

$$\alpha_1 \equiv R_1/R \ , \tag{41}$$

$$\alpha_2 \equiv R_2/R \ , \tag{42}$$

and

$$z_1 \equiv i\left(\frac{4\pi}{cR_{e1}}\right)\frac{ck}{\omega}$$

$$z_2 \equiv i\left(\frac{4\pi}{cR_{e2}}\right)\frac{ck}{\omega} \ . \tag{44}$$

To find k (or x) we must solve for f in the system of Equations 14 through 17 and set $E_{III\,z}$ at r = R equal to zero. That is we must solve the region III equation

$$J_0(x) + fn_0(x) = 0 \ , \tag{45}$$

where we use the relation

$$\frac{ck}{\omega} = \left(1 + \left(\frac{p\pi}{x}\frac{R}{L}\right)^2\right)^{-1/2} \ , \tag{46}$$

in z_1 and z_2 when we solve for f. If only membrane 2 were present then f would be

$$f = \frac{z_2(j_0(x\alpha_2))^2}{N_0(x\alpha_2)(J_1(x\alpha_2) - z_2J_0(x\alpha_2)) - N_1(x\alpha_2)J_0(x\alpha_2))} \ . \tag{47}$$

Recognizing that

$$J_1(y)N_0(y) - J_0(y)N_1(y) = 2/\pi y \ , \tag{48}$$

Equation 47 becomes

$$f = \frac{z_2(J_0(x\alpha_2))^2}{\frac{2}{\pi x\alpha_2} - z_2N_0(x\alpha_2)J_0(x\alpha_2)} \ . \tag{49}$$

Substituting Equation 49 into Equation 45 we find that the equation that must be solved to obtain the complex frequencies, for one membrane, is

$$J_0(x) + \frac{\pi}{2} x\alpha_2 z_2 J_0(x\alpha_2)(N_0(x)J_0(x\alpha_2) - N_0(x\alpha_2)J_0(x)) = 0 \quad (50)$$

3.2 AN APPROXIMATION FOR ONE AND TWO SHEET DAMPERS

An approximate solution to Equation 50 can be made by assuming that roots x_{np} with the damper (z_2 finite in Equation 50) are not much different than the roots without the damper x_n. That is we assume that

$$x_{np} = x_n^0 + \delta_{np} , \quad (51)$$

where δ_{np} is the small change from the zero order root. Under this first order assumption the δ_{np} for more than one damper would simply be the sum of the δ_{np} for each damper alone. Substituting Equation 51 into Equation 50 and using Equation 46 we find that

$$- J_1\delta_{np} + i\delta_{np}|z_0|S + igx_n^0|z_0| = 0 , \quad (52)$$

where

$$g(x) \equiv \pi/2\alpha J_0(x\alpha)(N_0(x)J_0(x\alpha) - N_0(x\alpha)J_0(x)) , \quad (53)$$

$$S = g(x_n^0)(1 + A_{np}) + x_n^0 \frac{\partial g}{\partial x_n^0} , \quad (54)$$

$$A_{np} = L_{np}(1 + L_{np})^{-1} , \quad (55)$$

$$L_{np} = \left(\frac{p\pi R}{x_n^0 L}\right)^2 , \quad (56)$$

$$|z_0| = \left(\frac{4\pi}{cR_e}\right)\frac{ck_0}{\omega_0} \quad (57)$$

$$\frac{ck_0}{\omega_0} = (1 + L_{np})^{-1/2} , \tag{58}$$

and where we have used the fact that

$$\frac{\partial J_0}{\partial x} = - J_1 . \tag{59}$$

The subscript 2 has also been dropped in Equation 50 since we need only consider one membrane in the present discussion. Letting

$$\delta_{np} = \delta_{np}^R + i\delta_{np}^I , \tag{60}$$

in Equation 52 while noting that $g(x_n^0)$ and S are real numbers we find that

$$\delta_{np}^I = \frac{x_n^0 |z_0| g(x_n^0) J_1(x_n^0)}{J_1^2(x_n^0) + |z_0|^2 S^2} , \tag{61}$$

and

$$\delta_{np}^R = - \frac{|z_0|^2 x_n^0 g(x_n^0)}{J_1^2(x_n^0) + |z_0|^2 S^2} . \tag{62}$$

From Equation 53 with the knowledge that x_n^0 is a root of J_0 it can easily be shown that

$$g(x_n^0) = \beta J_0^2(x_n^0 \alpha) N_0(x_n^0) , \tag{63}$$

and that

$$S = \beta J_0(x_n^0\alpha) [N_0(x_n^0) J_0(x_n^0\alpha)(1+A_{np}) + x_n^0(- 2\alpha N_0(x_n^0) J_1(x_n^0\alpha) + N_0(\alpha x_n^0) J_1(x_n^0) - N_1(x_n^0) J_0(x_n^0\alpha))] , \tag{64}$$

where

$$\beta \equiv \frac{\pi}{2} \alpha . \tag{65}$$

Note that $N_0(x_n^0)$ is almost equal to $J_1(x_n^0)$ in Equation 61 so that δ_{np}^I is positive definite.

Equations 61 and 62 are the equations which show how the wave number of the cavity mode changes when a damper shell is introduced into a cylindrical cavity. In order to investigate the modal damping we will first need to express the new modal frequency in terms of δ_{np}^I. We will then optimize the damping for a particular mode by finding what value of R_e makes the imaginary portion of the angular frequency, ω_{np}^I, a maximum for a given damper position. The frequency ω_{np}, for the n,p mode of a tank is

$$\left(\frac{\omega_{np}}{c}\right)^2 = \frac{x_n^2}{R^2} + \left(\frac{p\pi}{L}\right)^2 , \tag{66}$$

where we have used Equations 40 and 46. Substituting Equation 51 into 66 we find that

$$\omega_{np}^I = \frac{c}{R}\,\delta_{np}^I \left(1 + \left(\frac{p\pi R}{x_n^0 L}\right)^2\right)^{-1/2} . \tag{67}$$

We therefore see that maximizing the damping of the n,p mode requires maximizing δ_{np}^I. Taking the derivative of δ_{np}^I with respect to $|z_0|$ in Equation 61 and setting the result equal to zero we find the value of $|z_0|, |z_0|_M$ which makes δ_{np}^I a maximum:

$$|z_0|_M = \sqrt{J_1^2/S^2} . \tag{68}$$

Substituting Equation 70 into 69 we find the value of δ_{np}^I, $(\delta_{np}^I)_M$, which is maximum for a given position of the damper, namely

$$(\delta_{np}^I)_M = .5|g(x_n^0)/S|x_n^0 . \tag{69}$$

Note that (δ_n^I) will be zero (when E_z is zero) if the damper position is at the wall of the cylinder. That is when $J_0(\alpha x_n^0) = 0$. This result is in direct contrast to Equation 10 which implies that damping should be best at

the wall. As noted in Section 2, Equation 10 was derived under an erroneous assumption for the functional dependence of the field. Equation 69 is one of the equations we will be discussing in the next section. It, together with Equation 67, describe how the damping constant for the np mode depends upon position of the damper. Equation 68 contains the information necessary to determine the resistance of the damper sheet necessary for optimum damping. Using Equations 63, 68 and 61 we can put Equation 70 into a directly usable form

$$R_e = 120\pi\left(1 + \left(\frac{p\pi R}{x_n^0 L}\right)^2\right)^{-1/2} |J_1/S| \text{ (ohms)} . \qquad (70)$$

Equation 70 will also be discussed in the next section.

SECTION 4
RESULTS

In this section we will evaluate the optimum damping resistance from Equation 70 for a number of n,p modes as a function of damper position. We will also evaluate δ_{np} with the optimum resistance as a function of damper position, for a number of modes. The restriction on δ_{np} will be that it must be smaller than x^0_{np} for the damping constant to be meaningful. How the damping changes as the resistance deviates from the optimum value is also discussed. Finally a table of values of Q for modes, $5 \leq n \leq 1$ $0 \leq p \leq 10$, is constructed for a sheet damper at two positions, $\alpha = .8$ and $\alpha = .92$. These two positions correspond, roughly, to the sheet damper positions in the Physics International (PI) tank during the MRC March 1977 photon experiments.

Figures 2 through 4 are plots, for three representative values of p, of optimum resistance vs. damper position divided by the cylinder radius (α). The labels A to E correspond to n = 1 to 5 respectively. In general the resistances oscillate (except for n = 1) between zero and some larger value. Larger values of resistance occur for larger n's but, in general, decrease for increasing p. (n is associated with the number of nodes in the r direction and p with the number of nodes in the z direction.) The reduction of resistance with increasing p is associated with the fact that as p increases the electric field in the z direction becomes a smaller fraction of the total electric field so that a larger sheet current is necessary (smaller resistance) to obtain optimum damping. Figures 5 through 19 are a selection of δ^I_{np} vs. α. In conjunction with Equation 67 they can be used for designing a damper for modes

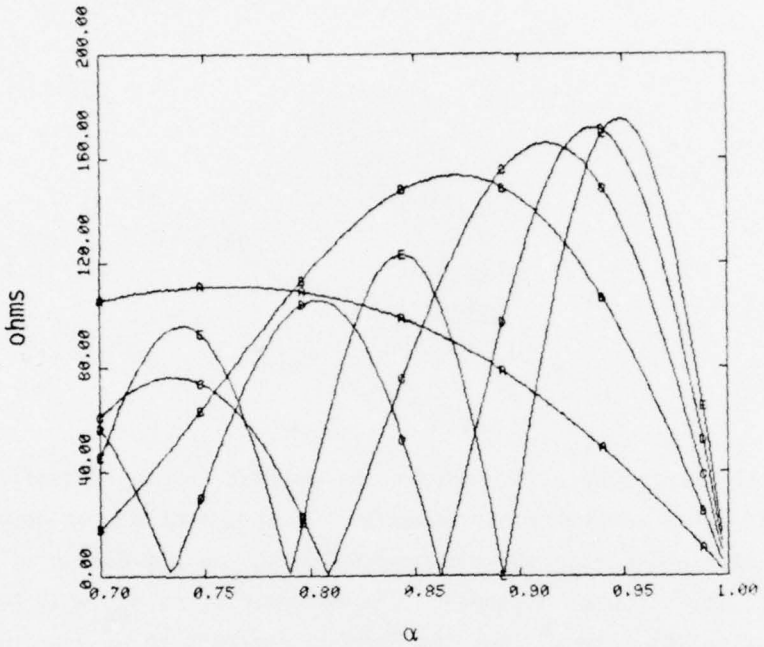

Figure 2. Optimum resistance vs. α, for $p = 0$, $n \leq 5$.

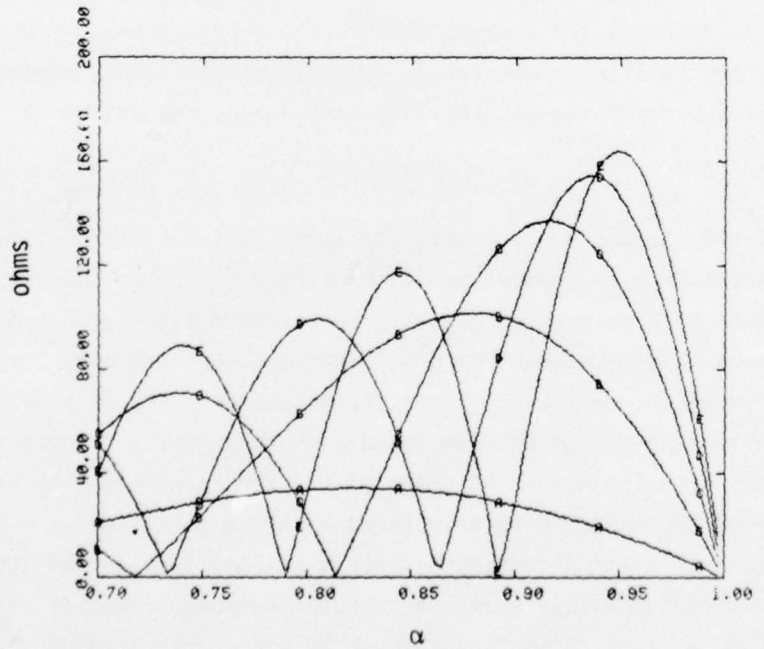

Figure 3. Optimum resistance vs. α, $p = 5$, $n \leq 5$.

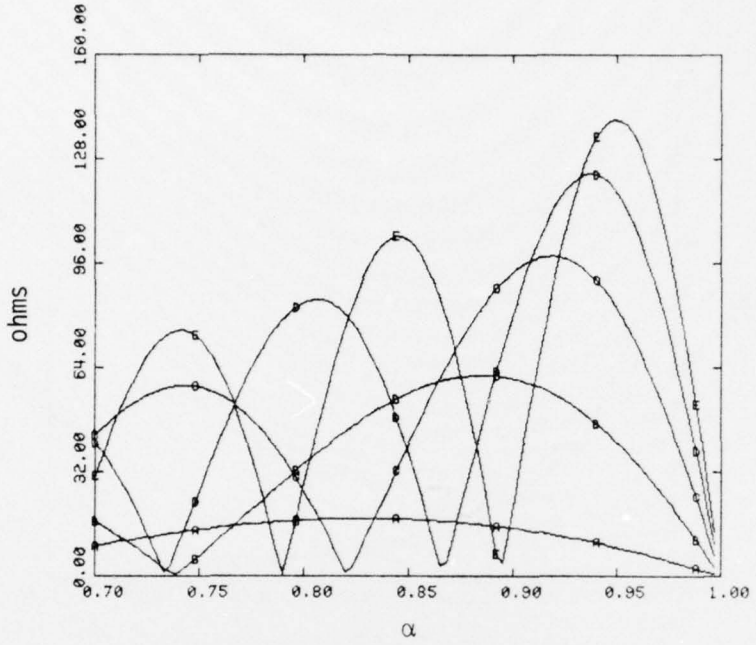

Figure 4. Optimum resistance vs. α, p = 10, n = 5.

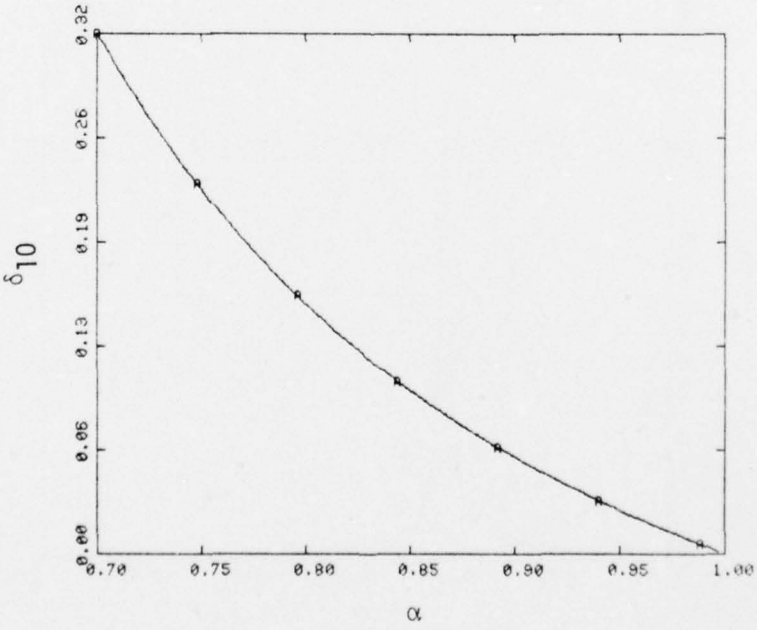

Figure 5. δ_{10}^{I} vs. α.

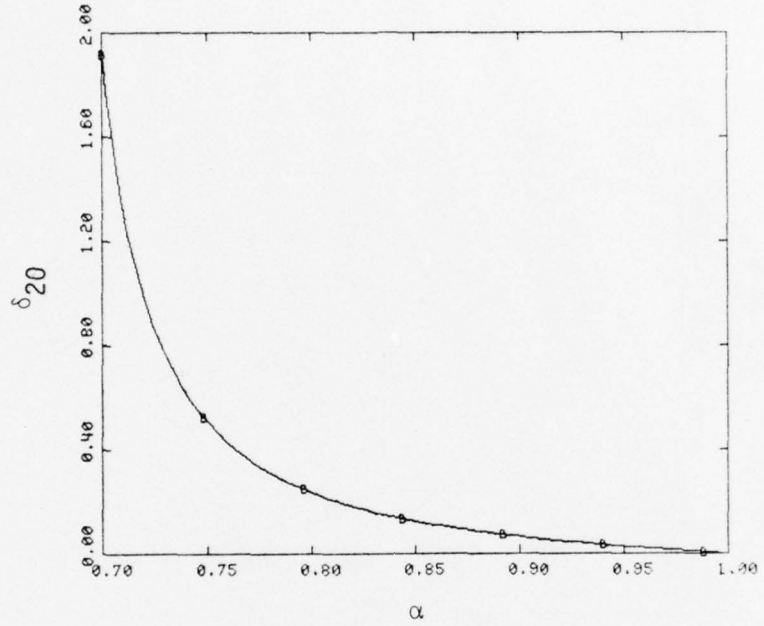

Figure 6. δ_{20}^{I} vs. α.

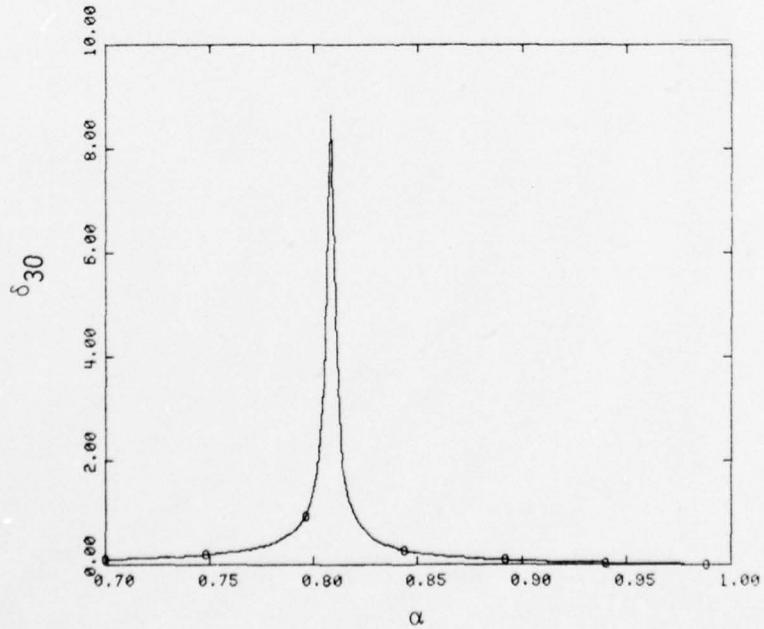

Figure 7. δ_{30}^{I} vs. α.

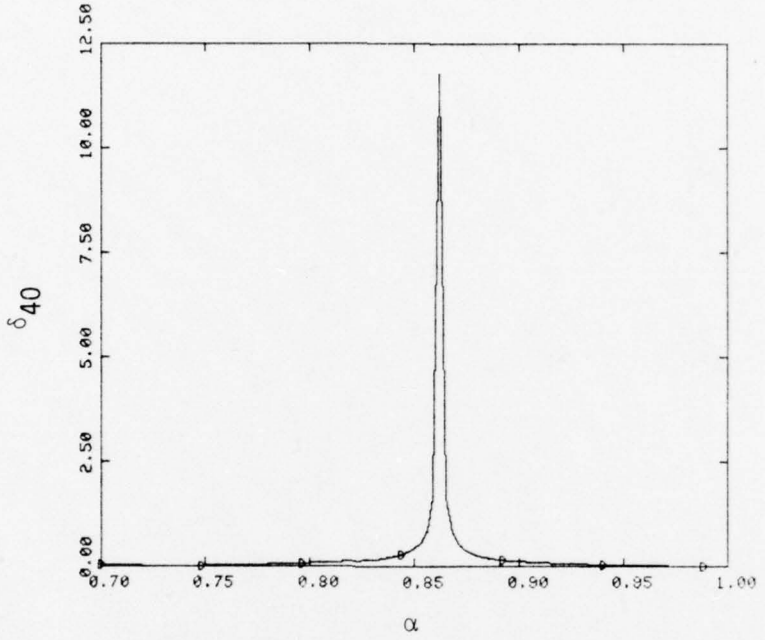

Figure 8. δ^{I}_{40} vs. α.

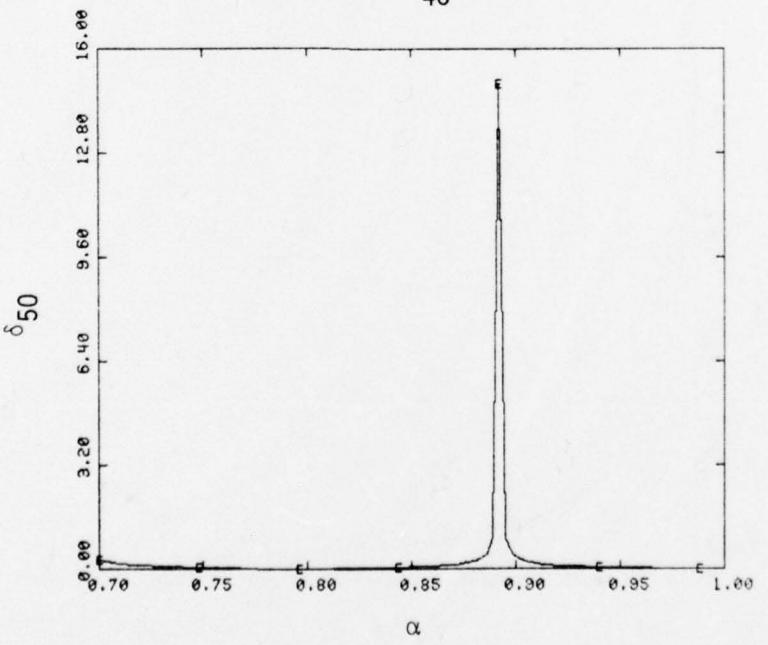

Figure 9. δ^{I}_{50} vs. α.

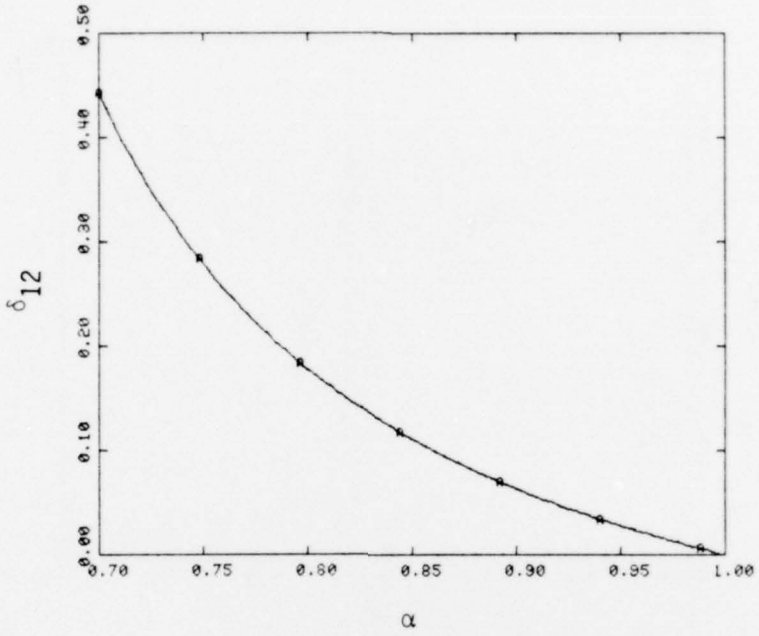

Figure 10. δ_{12}^{I} vs. α.

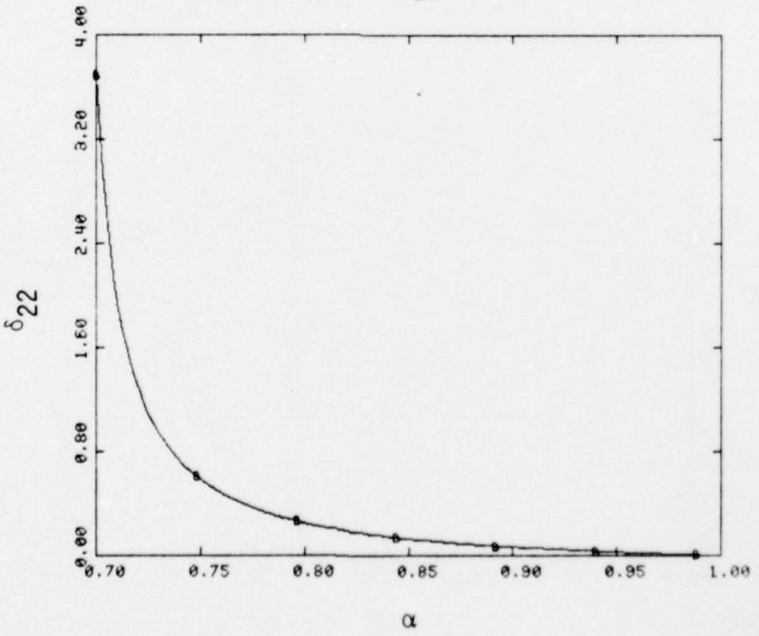

Figure 11. δ_{22}^{I} vs. α.

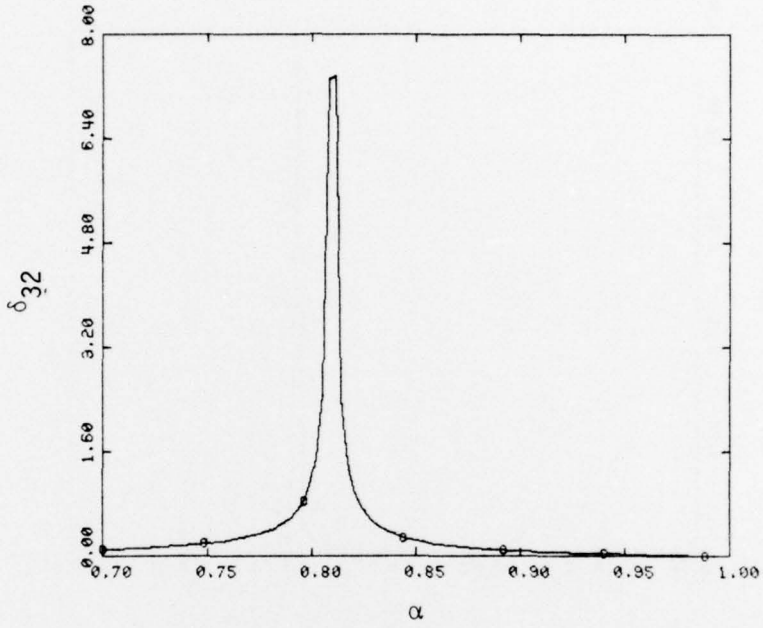

Figure 12. δ_{32}^{I} vs. α.

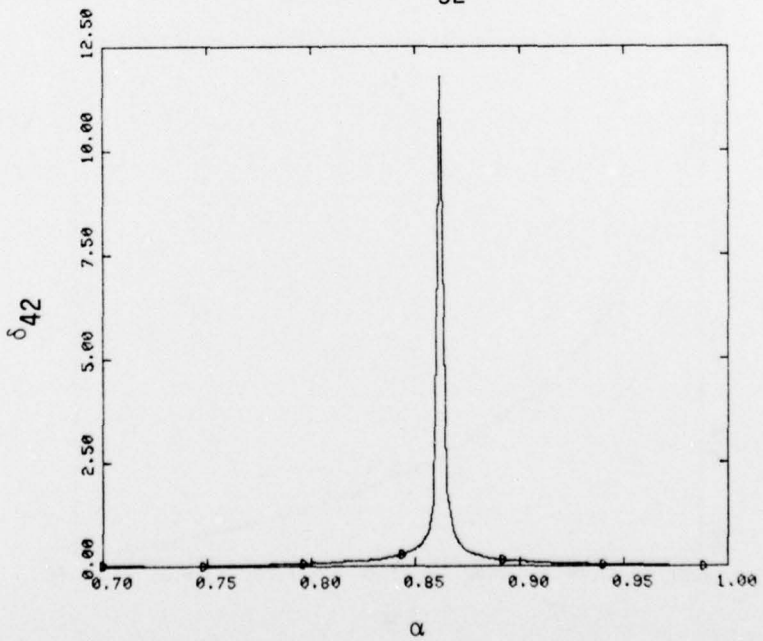

Figure 13. δ_{42}^{I} vs. α.

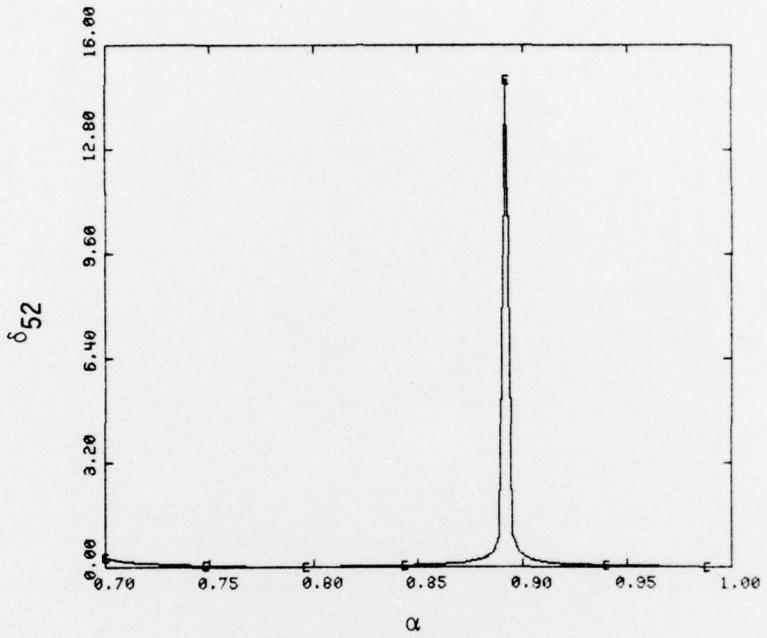

Figure 14. δ^I_{52} vs. α.

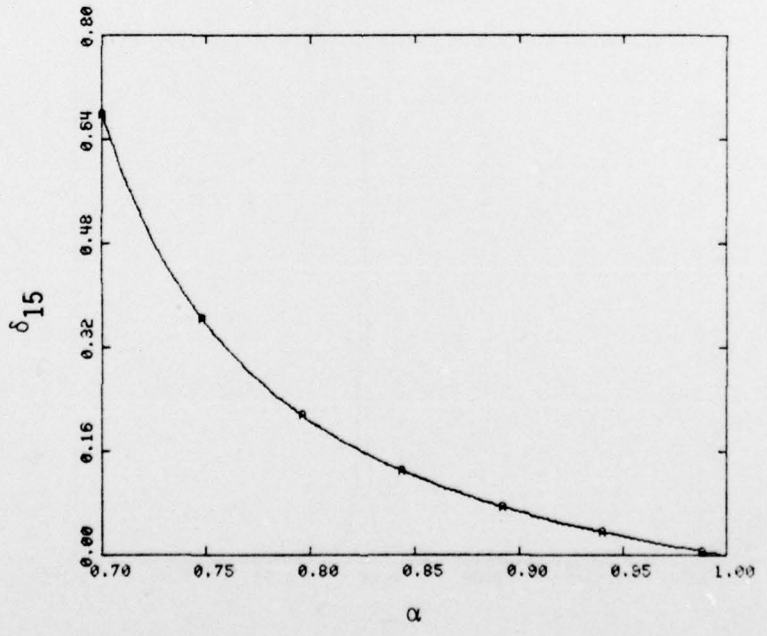

Figure 15. δ^I_{15} vs. α.

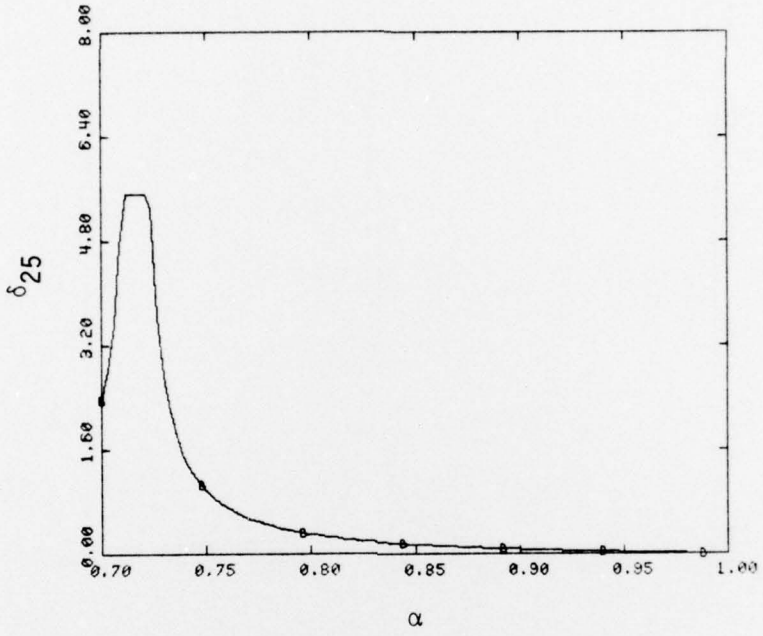

Figure 16. δ^I_{25} vs. α.

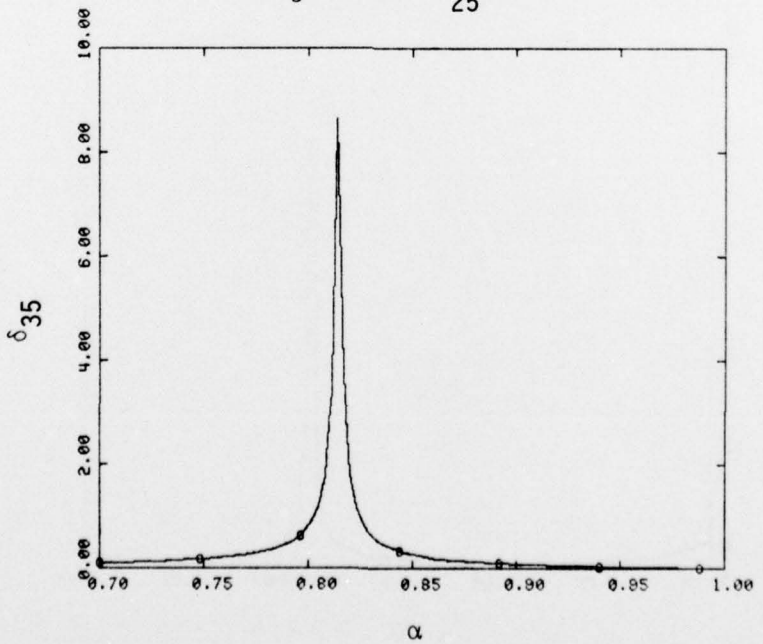

Figure 17. δ^I_{35} vs. α.

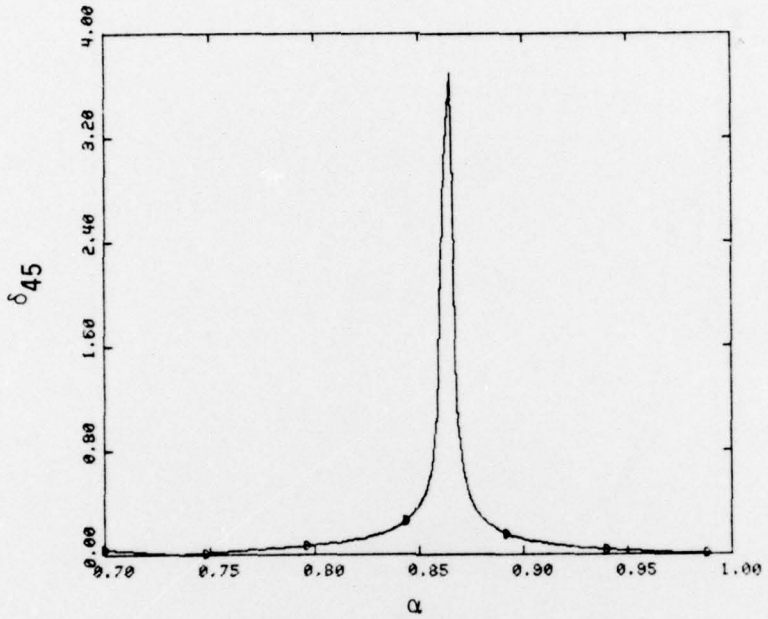

Figure 18. δ^{I}_{45} vs. α.

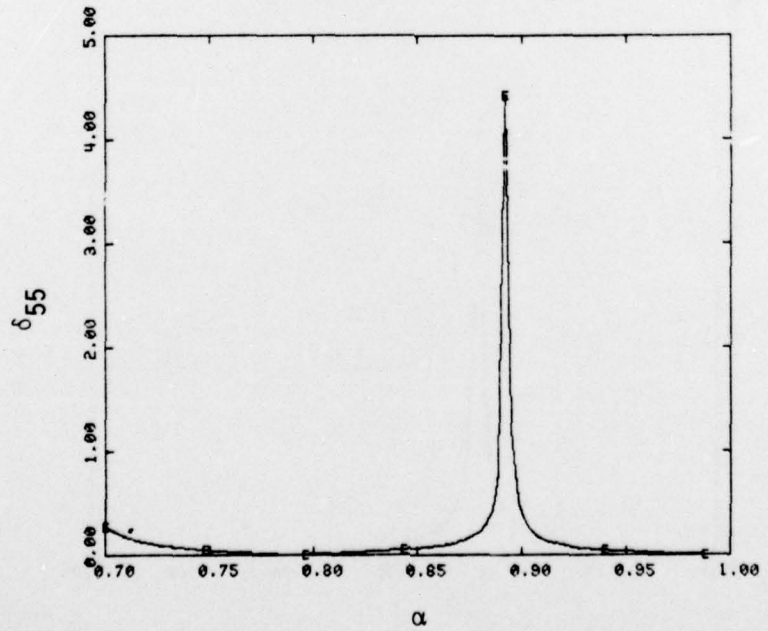

Figure 19. δ^{I}_{55} vs. α.

of a cylindrical cavity. The restriction on their use is that the figures are to be considered valid when $\delta_{np} < x_n^0$,

$$x_n^0 = 2.405,\ 5.520,\ 8.654,$$

$$x_n^0 \simeq n\pi - \pi/4 \ .$$

In Figures 5 through 19 the curves are plotted for a useful α range $.7 \leq \alpha \leq 1$. The curves are truncated for $\delta_{np} \sim x_n^0$ (for example δ_{25} in Figure 16 appears flat at the peak where $\delta_{25} \geq x_2^0$).

We now use Figures 2 through 19, and similar curves which are not presented, to construct a table of Q's for modes $1 \leq n \leq 5$ $0 \leq p \leq 10$ for a two sheet damper. To construct this table we first develop an expression for the Q for the n,p mode of a cylindrical cavity, Q_{np}. Beginning from Equation 67 the time, t_{np}, for the fields to decay to e^{-1} of their initial value is

$$t_{np} = \frac{R}{c\delta_{np}^I} (1 + L_{np})^{1/2} \ , \tag{71}$$

where L_{np} is given by Equation 56. Since the energy goes as the fields squared the time T_{np} (defined as the damping time) for the energy to decay to e^{-1} of its initial value is

$$T_{np} = .5\ t_{np} \ . \tag{72}$$

Thus from Equations 72 and 71, the expression for the period of the n,p mode

$$\tau_{np} = \frac{2\pi R}{cx_n^0} (1 + L_{np})^{-1/2} \ , \tag{73}$$

and the definition

$$Q_{np} \equiv \frac{T_{np}}{\tau_{np}} \ , \tag{74}$$

we have

$$Q_{np} = \frac{1}{4\pi} \frac{x_n^0}{\delta_{np}^I} (1 + L_{np}) \ . \qquad (75)$$

It is interesting to note that Q_{n0} is independent of the dimensions of the tank; Q_{n0} is dependent on the relative positions of the dampers, however.

We construct Table 1 by looking up values of δ_{np} in the figures adding them for the two damper sheets, at $\alpha = .8$ and .92, and inserting the values in Equation 75 where we take R/L = 1/3, roughly the dimensions of the PI vacuum tank. For example Q_0 is constructed in the following way: from Figure 5 δ_{10}^I for $\alpha = .8$ is .155 and δ_{10}^I for $\alpha = .92$ is .047. Adding the total δ_{10}^I is .20. Since L_{10} is zero

$$Q_{10} = \frac{1}{4\pi} \frac{(2.4)}{.2} = .95 \ .$$

Tables 4 and 5 are constructed by looking up the values for R_e on Figures 2 through 4 and similar figures not presented in this report. Tables indicates how valid the approximation $x_n^0/\delta_{np}^I > 1$ is. Table 3 indicates what the actual damping times are for the n,p modes of the PI tank ($R \cong 2$ m, $L \cong 6$ m) with optimum resistance dampers placed at $\alpha = .8$ and $\alpha = .92$.

We now consider the effect on δ_{np}^I for deviations away from the optimum resistance value. Our goal is to determine the effect on Q_{np} for a damper that is not optimized with respect to resistance. If U_{np} represents the ratio of the non-optimized δ_{np}^I to $(\delta_{np}^I)_M$ (Equation 69) and z_{np} represents the ratio of the non-optimized $|z_0|$ (see Equation 57) to $|z_0|_M$ (Equation 68) then by means of Equations 61, 68 and 69 we can show that

$$U_{np} = \frac{2 \ z_{np}}{1 + (z_{np})^2} \ . \qquad (76)$$

Figure 20 is a plot of Equation 76 and can be used to find Q_{np} for a damper of arbitrary resistance. For example if the actual resistance of the damper

Table 1. Q(n,p) for two damper sheets at α = .8 and α = .92.

n \ p	0	1	2	3	4	5	6	7	8	9	10
1	.956	1.09	1.49	2.15	3.08	4.28	5.74	7.47	9.46	11.7	14.2
2	1.54	1.57	1.67	1.83	2.06	2.35	2.70	3.11	3.59	4.13	4.73
3	.485	.511	.588	.715	.891	1.11	1.38	1.70	2.06	2.47	2.93
4	6.68	6.73	6.89	7.16	7.53	8.02	8.60	9.30	10.1	11.0	12.0
5	11.8	11.8	12.0	12.2	12.5	13.0	13.5	14.1	14.9	15.7	16.6

Table 2. X_n/δ^I_{np} for two damper sheets at α = .8 and α = .92.

n \ p	0	1	2	3	4	5	6	7	8	9	10
1	12.0	11.5	10.6	10.0	9.62	9.38	9.22	9.12	9.05	9.00	8.96
2	19.4	19.1	18.4	17.4	16.4	15.5	14.8	14.1	13.6	13.2	12.9
3	61.0	6.33	6.98	7.93	9.07	10.2	11.4	12.4	13.4	14.2	14.9
4	83.9	83.9	84.0	84.0	84.1	84.1	84.2	84.3	84.3	84.3	84.3
5	148	148	148	147	145	145	144	143	142	141	140

Table 3. Damping time T_{np} for TM cylindrical tank modes (in nanoseconds).

n \ p	0	1	2	3	4	5	6	7	8	9	10
1	33.3	34.8	39.2	45.7	53.6	62.3	71.6	81.2	91.0	101	111
2	23.4	23.5	23.7	24.2	24.9	25.9	27.1	28.4	30.0	31.7	33.5
3	4.70	4.91	5.53	6.51	7.76	9.24	10.8	12.5	14.3	16.2	18.1
4	47.5	47.6	48.2	49.2	50.5	52.1	54.0	56.1	58.5	61.1	63.8
5	66.3	66.4	66.7	67.3	68.0	69.0	70.1	71.5	73.0	74.7	76.5

Table 4. Optimum resistance (ohms) for sheet at $\alpha = .8$.

n \ p	0	1	2	3	4	5	6	7	8	9	10
1	109	94.6	70.9	53.1	41.5	33.7	28.4	24.4	21.4	19.1	17.1
2	116	113	102	89.9	77.1	65.1	56.6	56.6	42.6	38.4	33.9
3	17.4	16.1	19.2	19.3	21.3	24.6	24.5	24.5	27.2	26.1	27.1
4	105	105	104	103	101	98.4	96.1	93.3	90.0	87.2	83.7
5	30.6	33.8	30.3	33.2	32.7	28.9	31.3	30.5	26.8	28.8	25.2

Table 5. Optimum resistance (ohms) for sheet at $\alpha = .92$.

n \ p	0	1	2	3	4	5	6	7	8	9	10
1	62.9	56.2	45.5	35.6	28.8	24.2	20.5	17.8	15.8	14.1	17.1
2	130	127	120	110	99.4	90.1	80.7	73.0	66.7	60.6	33.9
3	165	163	159	153	145	137	128	120	66.7	105	27.1
4	160	160	156	154	149	143	138	132	112	119	83.7
5	115	119	114	116	113	107	107	103	124	95.4	25.2

is twice the optimum value then δ^I_{np} will be 80 percent of the optimum value. Since Q_{np} varies inversely as δ^I_{np}, Q_{np} will be 25 percent larger than optimum.

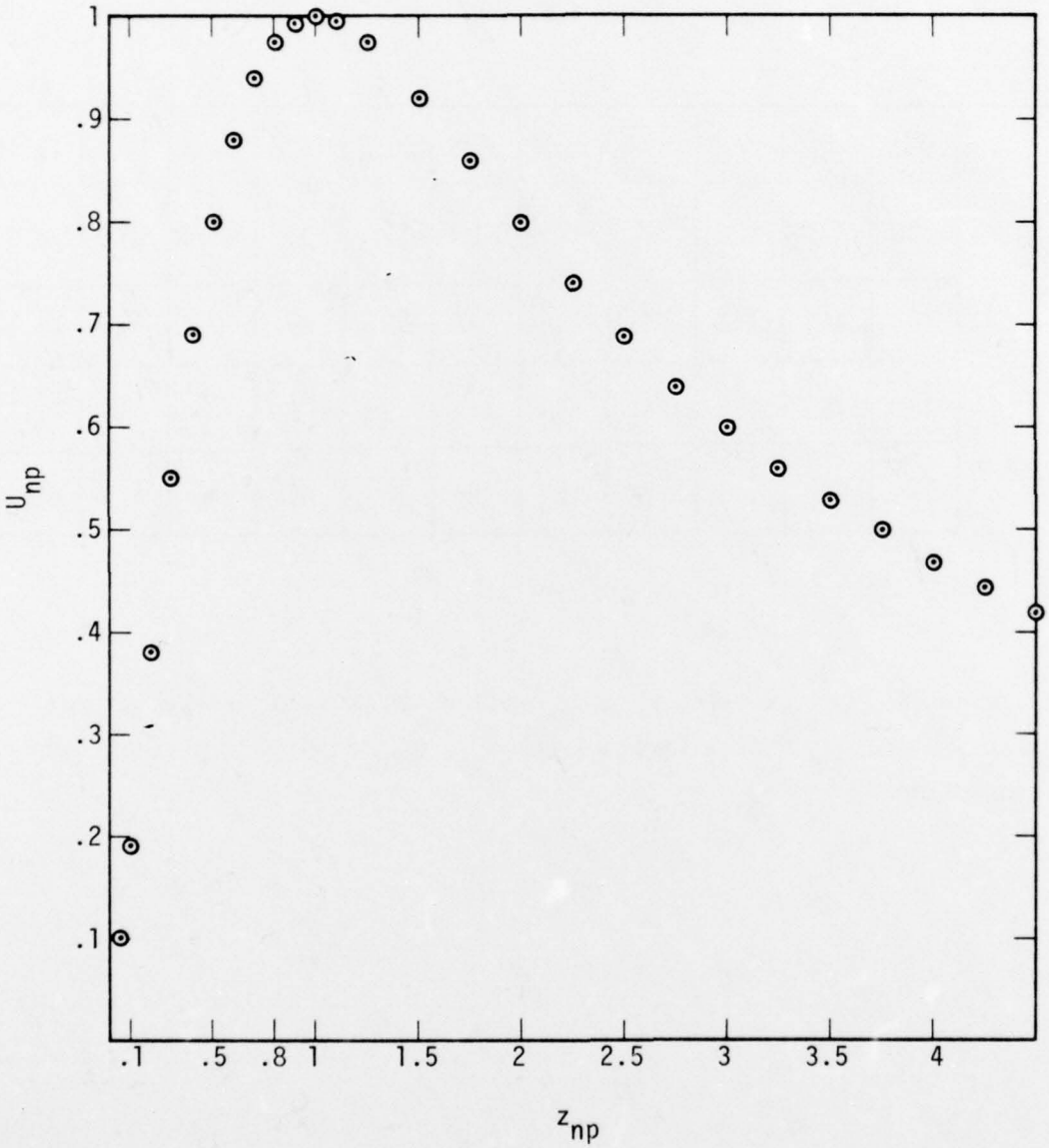

Figure 20. U_{np} vs. z_{np}.

SECTION 5
CONCLUSIONS

In Section 2 of this report we discussed the basic physical concepts underlying resistive sheet dampers by means of an oversimplified example. In Sections 3 and 4 we obtained the actual equations for two cylindrical dampers with no end caps. The equations were solved in first order. Table 1 indicates that many of the modes damp to e^{-1} of their initial value in about one modal period. Tables 4 and 5 indicate that, depending on the particular mode to be damped, the optimum sheet resistance can vary from 14 to 165 ohms. Although damping isn't a rapidly varying function of resistance it is still important, in building the damper, to have some idea what modes need to be damped.

The cylindrical sheet damper, with no end caps, becomes an increasingly poorer damper, as the frequency of the cavity increases (if the increasing frequency is due to an increasing number of nodes in the z direction only). As the frequency increases in this manner a smaller percentage of the electric field energy is associated with the z direction. Since it is the electric field in the z direction that causes the absorption of energy by the damper the cylindrical sheet damper with no end caps becomes a poorer damper. If one were interested in damping these higher frequency TM modes it would be necessary to add end caps to the damper.

REFERENCES

1. Messier, M. A., and K. S. Smith, A Theoretical Evaluation of the Membrane Damper Concept, Mission Research Corporation, MRC Photon Experiment Memo 5, January 7, 1977.

2. Messier, M. A., Spherical Cavity Damping—A Comparison of Spherical and Planer Model Predictions for a Single Membrane, Mission Research Corporation, MRC Photon Experiment Memo 4, January 3, 1977.

3. Seidler, W. A., Design of An Electromagnetic Damper for Resonant SGEMP Test Chambers, Simulation Physics, Inc. progress report PR 20026, August 1976.

4. Baum, C., A Technique for Simulating the System Generated Electromagnetic Pulse Resulting from an Exoatmospheric Nuclear Weapon Radiation Environment, Air Force Weapons Laboratory, Electronics Division, Sensor and Simulation Note 156, September 18, 1972.

5. Jackson, John D., Classical Electrodynamics, John Wiley & Sons, Inc., 1962.

DISTRIBUTION LIST

DEPARTMENT OF DEFENSE

Defense Documentation Center
Cameron Station
12 cy ATTN: TC

Director
Defense Nuclear Agency
ATTN: TISI, Archives
ATTN: DDST
2 cy ATTN: RAEV
3 cy ATTN: TITL, Tech. Library

Commander
Field Command
Defense Nuclear Agency
ATTN: FCLMC
ATTN: FCPR

Chief
Livermore Division, Fld. Command, DNA
Lawrence Livermore Laboratory
ATTN: FCPRL

Under Secretary of Def. for Rsch. and Engrg.
ATTN: S&SS (OS)

DEPARTMENT OF THE ARMY

Director
BMD Advanced Tech. Ctr.
ATTN: RDMH-O

Commander
Harry Diamond Laboratories
ATTN: DRXDO-RCC, John A. Rosado
ATTN: DRXDO-RCC, Raine Gilbert
ATTN: DRXDO-TI, Tech. Library
ATTN: DRXDO-NP

Commander
Picatinny Arsenal
ATTN: SMUPA
ATTN: SARPA

Commander
Redstone Scientific Information Ctr.
U.S. Army Missile Command
ATTN: Chief, Documents

Chief
U.S. Army Communications Sys. Agency
ATTN: SCCM-AD-SV, Library

Commander
U.S.Army Electronics Command
ATTN: DRSEL

DEPARTMENT OF THE NAVY

Chief of Naval Research
ATTN: Henry Mullaney, Code 427

Officer-In-Charge
Naval Surface Weapons Center
ATTN: Code WA501, Navy Nuc. Prgms. Off.

DEPARTMENT OF THE NAVY (Continued)

Director
Naval Research Laboratory
ATTN: Code 7750
ATTN: Code 5565, Jack Davis

Director
Strategic Systems Project Office
ATTN: NSP

DEPARTMENT OF THE AIR FORCE

AF Geophysics Laboratory, AFSC
ATTN: Charles Pike

AF Materials Laboratory, AFSC
ATTN: Library

AF Weapons Laboratory, AFSC
ATTN: SUL
2 cy ATTN: DYC
2 cy ATTN: NTS

Headquarters USAF/RD
ATTN: RDQSM

Commander
Rome Air Development Center, AFSC
ATTN: Edward A. Burke

SAMSO/DY
ATTN: DYS

SAMSO/MN
ATTN: MNNH
ATTN: MNNG

SAMSO/SK
ATTN: SKF

SAMSO/XR
ATTN: XRS

Commander In Chief
Strategic Air Command
ATTN: XPFS
ATTN: NRI-STINFO, Library

DEPARTMENT OF ENERGY

University of California
Lawrence Livermore Laboratory
ATTN: Tech. Info., Dept L-3

Los Alamos Scientific Laboratory
ATTN: Doc. Control for Reports Library

Sandia Laboratories
Livermore Laboratory
ATTN: Doc. Control for Theodore A. Dellin

Sandia Laboratories
ATTN: Doc. Control for 3141, Sandia Rpt. Coll.

OTHER GOVERNMENT AGENCY

NASA
Lewis Research Center
ATTN: Library
ATTN: N. J. Stevens
ATTN: Carolyn Purvis

DEPARTMENT OF DEFENSE CONTRACTORS

Aerospace Corporation
ATTN: Library
ATTN: Julian Reinheimer
ATTN: V. Josephson
ATTN: Frank Hai

AVCO Research & Systems Group
ATTN: Research Library, A830, Rm. 7201

The Boeing Company
ATTN: Preston Geren

University of California at San Diego
ATTN: Sherman De Forest

Computer Sciences Corporation
ATTN: Alvin T. Schiff

Dikewood Industries, Inc.
ATTN: Tech. Library
ATTN: K. Lee

EG&G, Inc.
Albuquerque Division
ATTN: Technical Library

Ford Aerospace & Communications Corp.
ATTN: Library
ATTN: Donald R. McMorrow, MS G30

General Electric Company
Space Division
Valley Forge Space Center
ATTN: Joseph C. Peden, VFSC, Rm. 4230M

General Electric Company
TEMPO-Center for Advanced Studies
ATTN: DASIAC
ATTN: William McNamara

Hughes Aircraft Company
ATTN: Tech. Library

Hughes Aircraft Company, El Segundo Site
ATTN: Edward C. Smith, MS A620
ATTN: William W. Scott, MS A1080

IRT Corporation
ATTN: Technical Library
ATTN: Dennis Swift

DEPARTMENT OF DEFENSE CONTRACTORS (Continued)

JAYCOR
ATTN: Eric P. Wenaas
ATTN: Library

JAYCOR
ATTN: Robert Sullivan

Johns Hopkins University
Applied Physics Laboratory
ATTN: Peter E. Partridge

Kaman Sciences Corporation
ATTN: Library
ATTN: Jerry I. Lubell
ATTN: W. Foster Rich

Lockheed Missiles & Space Co., Inc.
ATTN: Dept. 85-85

McDonnell Douglas Corporation
ATTN: Stanley Schneider

Mission Research Corporation
ATTN: Roger Stettner
ATTN: Robert Marks
ATTN: Conrad L. Longmire
5 cy ATTN: Technical Library

Mission Research Corporation-San Diego
ATTN: Victor A. J. Van Lint
ATTN: Library

R & D Associates
ATTN: Technical Library
ATTN: Leonard Schlessinger

Rockwell International Corporation
ATTN: Technical Library

Science Applications, Incorporated
ATTN: William L. Chadsey

Spire Corporation
ATTN: Roger G. Little

Systems, Science and Software, Inc.
ATTN: Technical Library
ATTN: Andrew R. Wilson

TRW Defense & Space Sys. Group
ATTN: Tech. Info. Center/S-1930
2 cy ATTN: Robert M. Webb, R1-2410